ELSEVIER

Contents lists available at ScienceDirect

Solid State Ionics

journal homepage: www.elsevier.com/locate/ssi



Influence of graphene on the magnetic properties of nickel ferrite nanoparticles



Monica Sorescu^{a,*}, Matthew Knauss^a, Alice Perrin^{b,c}, Michael McHenry^b

- ^a Duquesne University, Department of Physics, Fisher Hall, Pittsburgh, PA 15282, United States of America
- b Carnegie Mellon University, Department of Materials Science and Engineering, Roberts Hall, Pittsburgh, PA 15213, United States of America
- c Massachusetts Institute of Technology, Department of Materials Science and Engineering, Building 8, Cambridge, MA 02142, United States of America

ARTICLE INFO

Keywords:
Ferrites
Mössbauer spectroscopy
Magnetic properties

ABSTRACT

Nickel ferrite nanoparticles were subjected to mechanochemical activation for ball milling times ranging from 0 to 12 h. The milling was performed with and without the addition of equimolar concentrations of graphene nanoparticles. Characterization of resulting nano-powders was undertaken by Mössbauer spectroscopy and magnetic measurements. The hyperfine magnetic field was studied as function of milling time for octahedral and tetrahedral sites. An additional quadrupole split doublet represented the occurrence of superparamagnetic particles in the as-obtained and milled specimens. A new phase was obtained in the graphene-milled set of samples, which could be assigned to carbon-rich particles. The degree of inversion and canting angle were derived from the Mössbauer measurements and studied as function of ball milling time. The degree of inversion was found to decrease with milling time, especially for the set without graphene and evidenced a transition from inverse to normal spinels. The canting angle decreased with time for the graphene milled nanoparticles. The recoilless fraction was determined as function of milling time and was consistent with the observation - for the first time in literature - of a distribution of recoilless fractions in the studied specimens. The saturation magnetization, remanence magnetization and coercive field were derived from the hysteresis loops, recorded at 5 K and 5 T. The zero-field-cooling-field-cooling measurements were obtained in a magnetic field of 200 Oe and the blocking temperature was determined. Our results show new features of the behavior of nickel ferrite nanoparticles under mechanochemical activation with and without graphene.

1. Introduction

Nanoparticles possessing magnetic properties introduced in a non-magnetic graphene host combine both the benefits of the unique properties of graphene and magnetization. When these magnetic particles are inserted in a graphitic matrix, the carbon layers isolate the particles magnetically from each other, providing protection against oxidation. Alternatively, the incorporation of carbon in ferrite nanoparticles lattice may give rise to nanocomposite and new hybrid materials. These can open up new prospects in bioengineering and energy applications, such as controlled drug delivery, magnetic recording media, magnetic toners, magnetic resonance imaging, ferrofluids, as well as in electrochemical energy storage and supply [1–19].

Nickel ferrite (space group Fd-3m) has been the subject of intense investigations due to its outstanding magnetic and electric properties. The compound Ni ferrite has an inverse spinel cubic structure. The crystal includes two intertwining sub-lattices A and B which are

tetrahedrally and octahedrally coordinated, respectively. The tetrahedral site is occupied by ${\rm Fe}^{3+}$ ions while the B site consists of an equal distribution of ${\rm Fe}^{3+}$ and ${\rm Ni}^{2+}$ ions. The ferrimagnetic nature arises from the anti-parallel alignment of spins of unequal magnitude at the A site and the B site [20–30].

Nickel ferrite is a major candidate for telecommunications, microwave devices, and sensor applications because of its high resistivity and moderate magnetization [31–39]. The dielectric and magnetic properties of such ferrites depend strongly on preparation methodology and distribution of cations at the tetrahedral (A) and octahedral (B) sites in the lattice.

In this paper we report novel investigations of nickel ferrite in the nanoparticle form: (i) the behavior of nickel ferrite during mechanochemical activation; (ii) the behavior of graphene during high-energy ball milling with nickel ferrite nanoparticles; (iii) the effect of graphene and milling on the degree of inversion and canting angle; and (iv) the effect of milling on the recoilless fraction of nickel ferrite nanoparticles.

^{*} Corresponding author at: Duquesne University, Department of Physics, 600 Forbes Avenue, 309 B Fisher Hall, Pittsburgh, PA 15282, United States of America. E-mail address: sorescu@duq.edu (M. Sorescu).

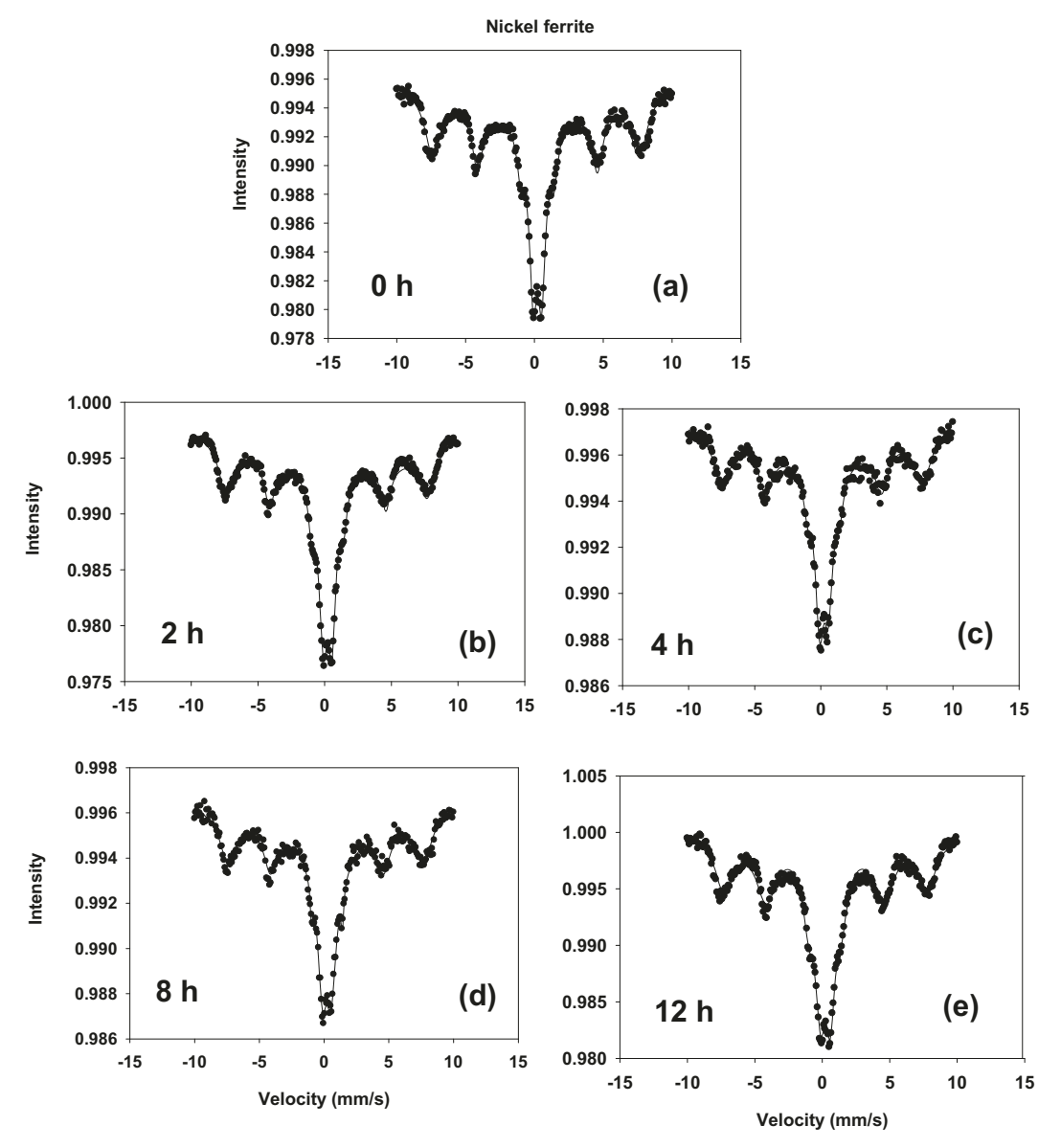


Fig. 1. (a)-(e) displays the Mössbauer spectra collected after ball milling for 0-12 h.

2. Materials and methods

Nickel ferrite nanoparticles (Alfa Aesar, 50 nm particle size) were exposed to mechanochemical activation by high-energy ball milling for time intervals of 0–12 h, with and without equimolar mixtures of zero-dimensional graphene (SkySpring Nanomaterials, 1–5 nm particle size).

Samples of precursors were introduced in a SPEX 8000 mixer mill and ground for time periods ranging from 0 to 12 h. The 8000M Mixer/Mill is a high-energy ball mill that grinds up to 0.2–10 g of dry, brittle samples. The vial, which contains a sample and one or more balls, is shaken in a complex motion that combines back-and-forth swings with short lateral movements. The clamp's motion develops strong G-forces in the vial, to pulverize the toughest rocks, slags and ceramics. In our experiments the powder: ball mass ratio was 1:5.

The room-temperature transmission Mössbauer spectra were

recorded using a SeeCo constant accelerator spectrometer equipped with a 25 mCi 57 Co gamma ray source. Hysteresis loop measurements were recorded with a Quantum Design SQUID magnetometer at a temperature of 5 K and an applied magnetic field of 5 T, while the zero-field-cooling-field-cooling was performed at 200 Oe (1 Oe = 10^{-4} T) and a temperature interval of 5–300 K.

3. Results and discussion

Fig. 1(a)–(e) shows the room temperature Mössbauer spectra recorded in the transmission geometry using gamma radiation emitted by a 57 Co source diffused in a Rh matrix. The spectrometer was operated in the constant acceleration mode and the spectra for nickel ferrite were taken after 0 to 12 h of ball milling time. All spectra, both as-obtained and processed, were fitted with 2 sextets, corresponding to the

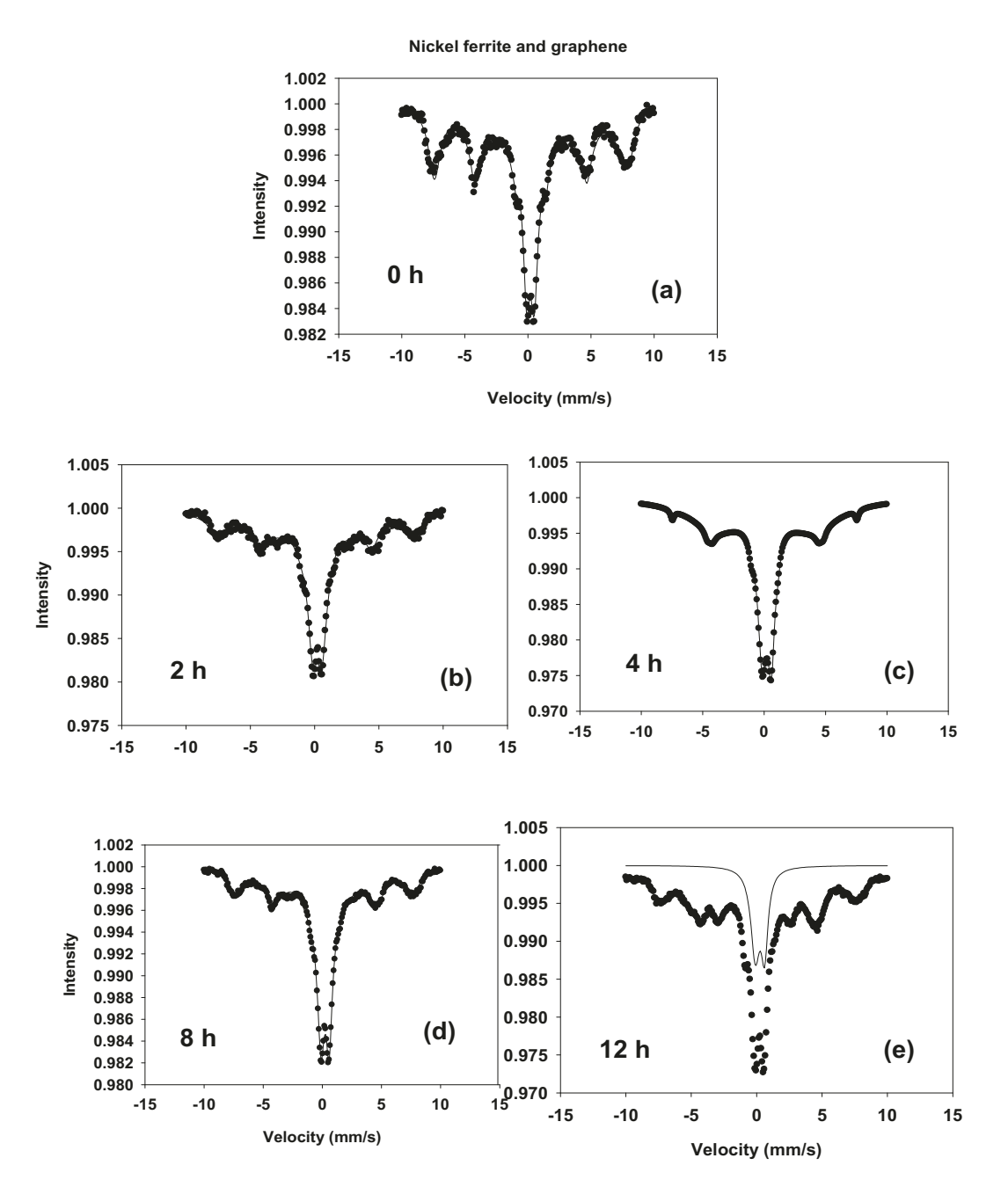


Fig. 2. (a)—(e) displays the Mössbauer spectra collected after ball milling for 0–12 h with graphene. Spectrum in Panel (e) emphasizes the contribution of the doublet. Additional resonances appear in the spectrum.

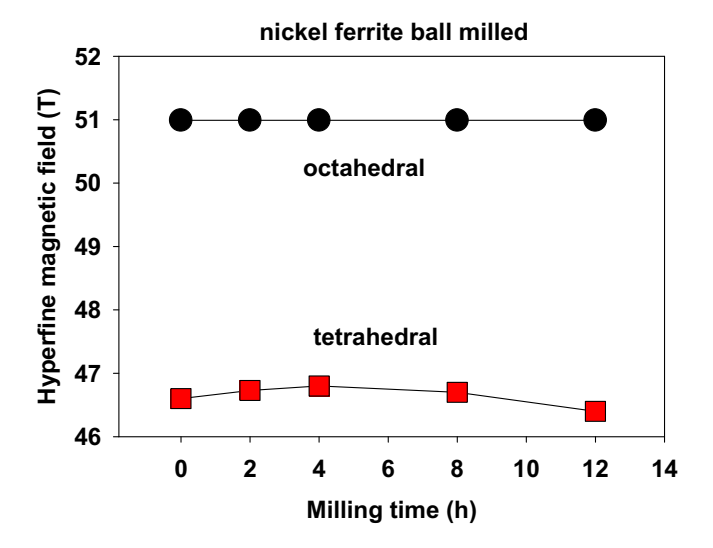
tetrahedral and octahedral magnetic sublattices, as well as a quadrupole split doublet, which is indicative of the occurrence of superparamagnetism in the nanoparticles system (\sim 30% abundance).

Fig. 2(a)–(e) displays the Mössbauer spectra collected after ball milling for 0–12~h, with graphene nanoparticles added to the milling powders of nickel ferrite.

The hyperfine parameters are plotted in Fig. 3. It can be observed that a new sextet, with a lower value of the hyperfine magnetic field, appears in the spectrum of ferrite milled with graphene. This can be assigned to Fe atoms having an increased number of carbon atoms as nearest neighbors.

The NiFe₂O₄ structure can be written as $(Ni_{1-\lambda}Fe_{\lambda})[Ni_{\lambda}Fe_{2-\lambda}]O_4$, where λ is the fraction of the A sites occupied by Fe^{3+} cations, known as the degree of inversion. This parameter is given by the formula: $I_A/I_B = f_A/f_B \, x \, \lambda/(2-\lambda)$, where I are the areal intensities of the two sextets, $f_B/f_A = 0.94$ at room temperature are the recoilless fractions [38], while the degree of inversion takes values $\lambda = 0$ for a normal spinel, $\lambda = 1$ for an inverse spinel and $\lambda = 2/3$ for a random distribution.

It can be seen in Fig. 4 that the degree of inversion λ decreases from the value of one to 0.15 after 12 h of milling, such that the material can be designed to take all forms from inverse to normal spinel structures. If graphene is added to the milling powders, the degree of inversion



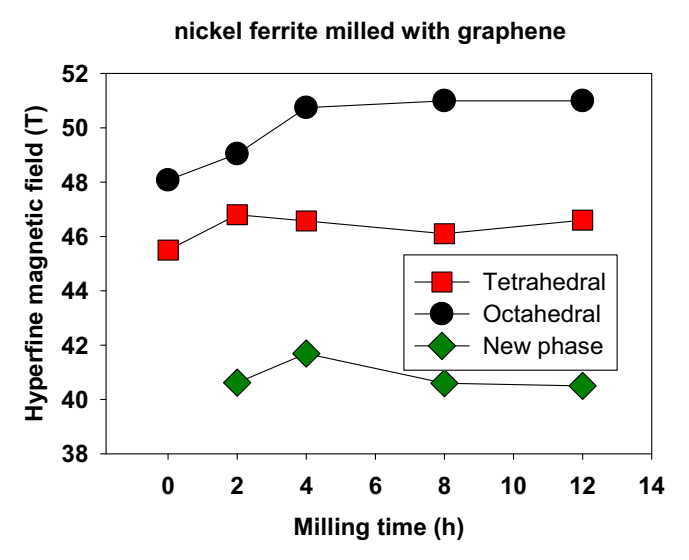
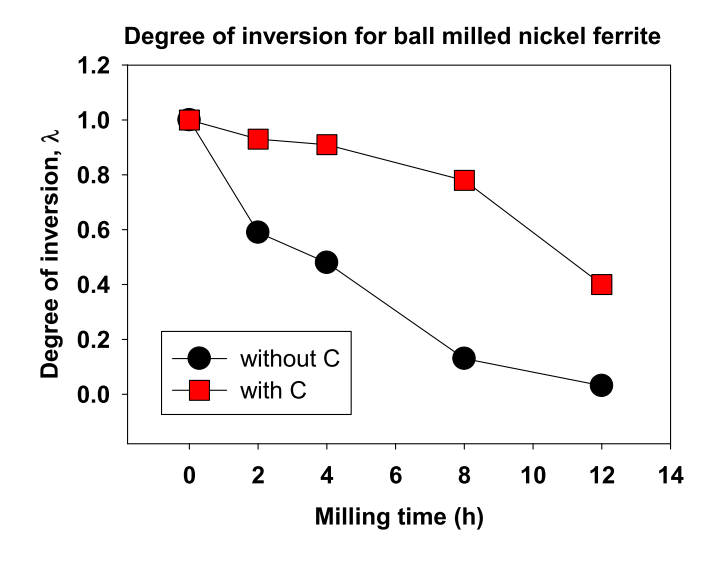


Fig. 3. Hyperfine magnetic fields as function of ball milling times for nickel ferrite, with and without graphene additions during mechanochemical activation.

decreases again, but to a lesser extent, such that mixed spinels are typically obtained.

Another parameter that can be derived from the Mössbauer spectra of the nickel ferrite is the canting angle, which is the average angle between the direction of the hyperfine magnetic field and the direction of propagation of the gamma radiation. The canting angle is given by the formula: $\theta = \arcsin[3/2(I_2/I_1)]/[1 + 3/4(I_2/I_1)]$. It can be seen in Fig. 4 that the canting angle of milled nickel ferrite stays constant at about 41.46° , while the presence of graphene lowers its value to 25.2° . This means that milling with graphene tends to align the hyperfine field of the ferrite nanoparticles along the direction of gamma ray propagation.

Fig. 5(a)–(e) displays the composite Mössbauer spectra of the nickel ferrite system for the 0–12 h ball milling time. These spectra were recorded simultaneously with a stainless steel etalon, whose signature in the composed spectrum is a singlet with a negative isomer shift of



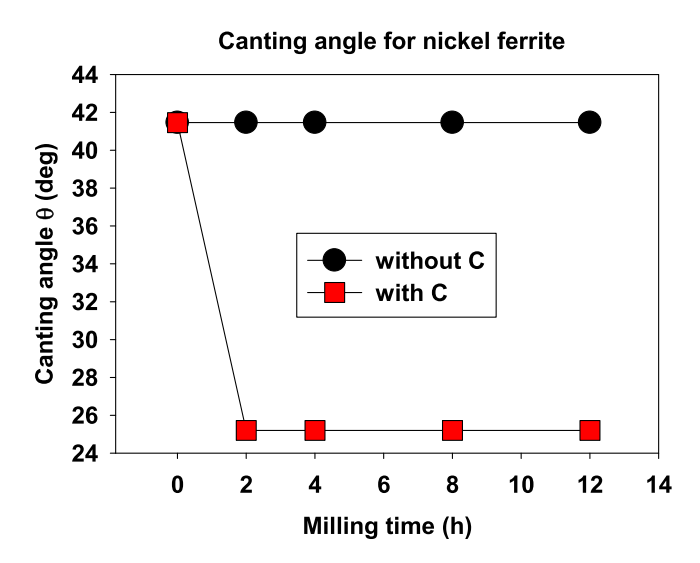


Fig. 4. Degree of inversion and canting angle for nickel ferrite.

-0.27 mm/s (Fig. 6). Following our procedure outlined in [35], the values of the recoilless fraction f_1 can be obtained from the relative areas of the subspectra and some simple chemical arguments:

$$f_1 = f_e(N_e/N_1)(\mu_1/\mu_e)(m_e/m_1)(A_1/A_e), \tag{1}$$

where f_e is the recoilless fraction of the stainless steel etalon (0.7), N_e and N_1 are the numbers of iron nuclei per formula unit for etalon and ferrite, μ_1 and μ_e are the molar masses for the sample and etalon, m_e and m_1 are the masses corresponding to the etalon and sample, and A_1 and A_e are the resonant areas for the sample and etalon, respectively.

Applying this methodology, the recoilless fraction values averaged at about 0.6, value which is consistent with a reduced contribution of particles at the nanoscale. The Mössbauer spectra were fitted with a singlet for the stainless steel etalon and a hyperfine magnetic field distribution for the ferrite. The probability distribution is given in Fig. 7(a)–(d) for 2–12 milling hours. It can be inferred that the hyperfine magnetic field distribution corresponds to a distribution of particle sizes produced by milling, which in turn gives rise to a

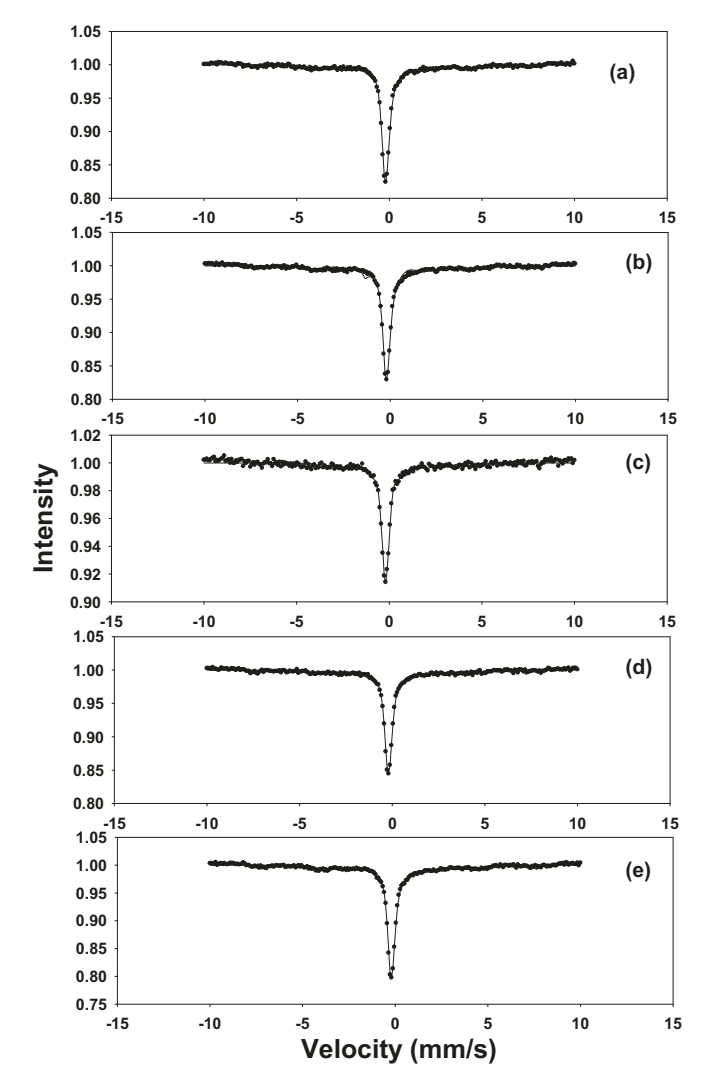


Fig. 5. Mössbauer spectra recorded simultaneously with the stainless steel etalon after various milling times (a)–(e).

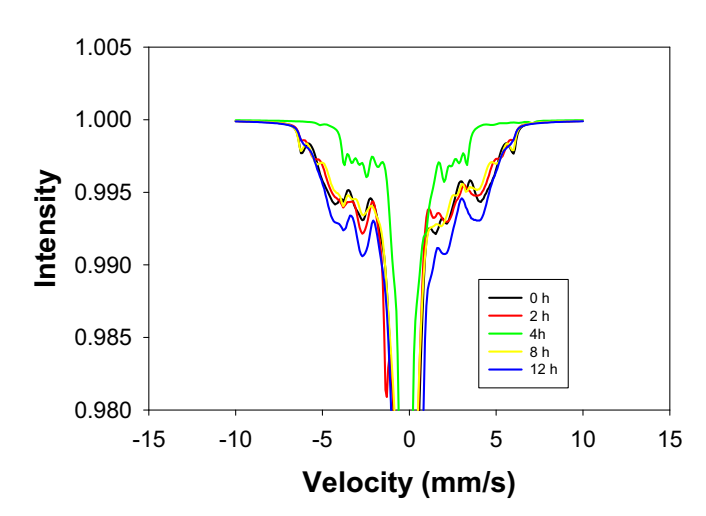


Fig. 6. Expanded Mössbauer spectra for the nickel ferrite nanoparticles system and stainless steel etalon.

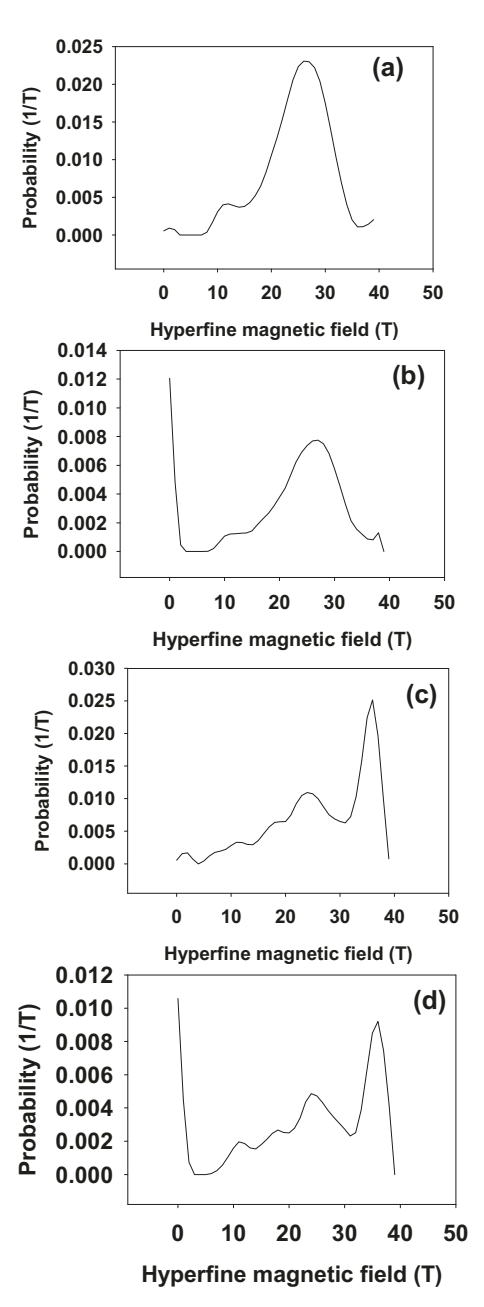
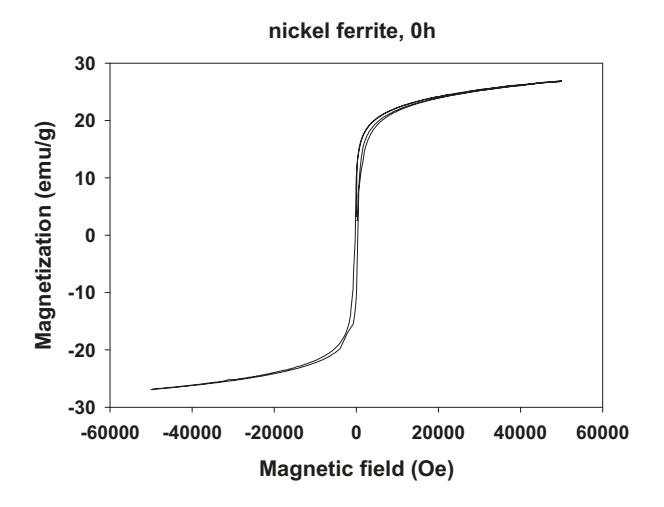


Fig. 7. Hyperfine magnetic field distribution for the nickel ferrite (a)-(d).

distribution of recoilless fraction values, where the f factor tends to be lower for smaller nanoparticles and long milling times. To our best knowledge, it is for the first time in literature that a *distribution* of recoilless fraction values is evidenced.

In what follows we would like to correlate the local-probe information obtained from Mössbauer spectroscopy with the global information inferred from magnetic measurements. Fig. 8 plots the hysteresis loops recorded at 5 K and 5 T for the samples milled at 0 h and 12 h. The saturation magnetization stays the same, but the remanence magnetization increases from 4.28 to 13.8 emu/g. Moreover, the coercive field increases boldly, from 1428 to 3000 Oe.

The zero-field-cooling-field cooling (ZFC-FC) experiments were performed in an applied magnetic field of 200 Oe in the temperature



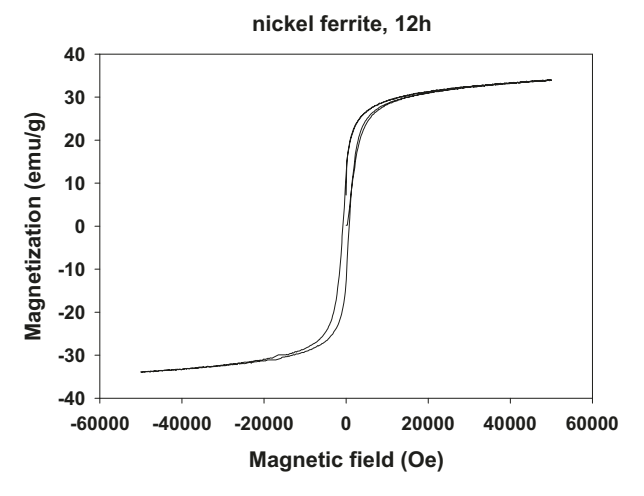


Fig. 8. Hysteresis loops of the nickel ferrite after milling for 0 and 12 h.

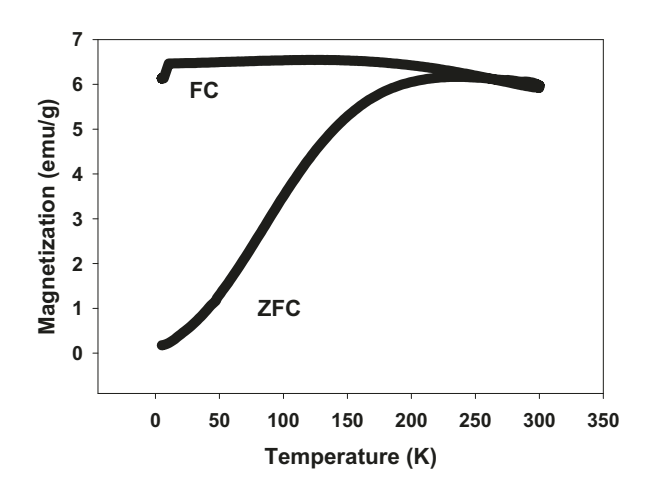
interval 5–300 K and shown in Fig. 9 for 0 h and 12 h of milling. The maximum value on the ZFC curve yielded the blocking temperature, which was found to increase from 225 K for the as-obtained specimen to 250 K for the sample milled at 12 h with graphene. Indeed, we showed recently that the addition of graphene in the milling powder was able to change the blocking temperature of a zinc ferrite system of nanoparticles [37].

4. Conclusions

In this work we successfully synthesized nickel ferrite nanoparticles, with and without graphene, by high energy ball milling. The main results obtained from the Mössbauer spectroscopy and magnetism study are as follows:

- (i) The hyperfine magnetic field of the tetrahedral and octahedral sites was studied as function of ball milling time. A quadrupole doublet was resolved due to the presence of superparamagnetic particles in the system. A third sextet was obtained for the sample rich in graphene and was assigned to Fe atoms having an increased number of carbon atoms as nearest neighbors.
- (ii) The study of the degree of inversion as function of ball milling time demonstrated that spinels with inversions between 1 and 0 can be engineered, while the degree of inversion for the sample with

nickel ferrite, 0h, zfc





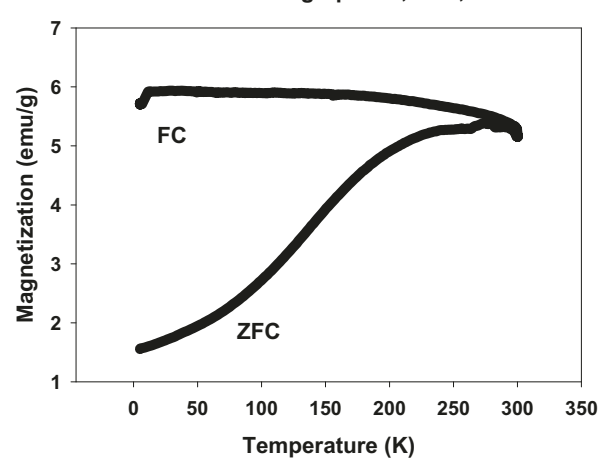


Fig. 9. ZFC-FC curves for the nickel ferrite at 0 h and ferrite with graphene at $12\ h.$

graphene showed a less abrupt decline.

- (iii) The canting angle decreased when the content of graphene was increased.
- (iv) The distribution of the hyperfine magnetic field was correlated to a distribution of particle sizes, which in turn was related to a distribution of recoilless fractions.
- (v) The coercivity was determined from the hysteresis loops and found to triple as function of ball milling time.
- (vi) The blocking temperature was derived from ZFC and found to depend on the presence of graphene in the system.

Author statement

The author certifies that all four co-authors contributed to the work load as described in the present paper.

Declaration of competing interest

There are no conflicts of interest known for this paper.

Acknowledgments

This work was supported by the National Science Foundation, US under grants DMR-0854794, DMR-1002627 and DMR-1709247.

References

- M. DeGraef, M.E. McHenry, Structure of Materials, 2nd edition, Cambridge University Press, 2012 (ISBN 9781107005877).
- [2] Z.Z. Lazarevic, C. Jovalekic, A. Recnik, V.N. Ivanovski, A. Milutinovic, M. Romcevic, M.B. Pavlovic, B. Cekic, N.Z. Romcevic, Preparation and characterization of spinel nickel ferrite obtained by the soft mechanochemically assisted synthesis, Mater. Res. Bull. 48 (2013) 404–415.
- [3] Z.Z. Lazarevic, A.N. Milutinovic, C.D. Jovalekic, V.N. Ivanovski, N. Daneu, I. Madarevic, N.D. Romcevic, Spectroscopy investigation of nanostructured nickelzinc ferrite obtained by mechanochemical synthesis, Mater. Res. Bull. 63 (2015) 230–247
- [4] A.S. Albuquerque, J.D. Ardisson, W.A.A. Macedo, J.L. Lopez, R. Paniago, A.I.C. Persiano, Structure and magnetic properties of nanostructured Ni-ferrite, J. Magn. Magn. Mater. 226-230 (2001) 1379–1381.
- [5] R. Malik, S. Annapoorni, S. Lamba, V.R. Reddy, A. Gupta, P. Sharma, A. Inoue, Mössbauer and magnetic studies in nickel ferrite nanoparticles: effect of size distribution, J. Magn. Magn. Mater. 322 (2010) 3742–3747.
- [6] C.M. Kale, P.P. Bardapurkar, S.J. Shukla, K.M. Jadhav, Mössbauer spectral studies of Ti⁴⁺ substituted nickel ferrite, J. Magn. Magn. Mater. 331 (2013) 220–224.
- [7] A.M. Gismelseed, A.A. Yousif, Mössbauer study of chromium-substituted nickel ferrites, Physica B 370 (2005) 215–222.
- [8] B. Ndlovu, J.Z. Msomi, T. Moyo, Mössbauer and electrical studies of $\rm Ni_xCo_{1.x}Fe_2O_4$ nanoparticles, J. Alloys Compd. 745 (2018) 187–195.
- [9] S.K. Gore, S.S. Jadhav, U.B. Tumberphale, S.M. Shaikh, M. Naushad, R.S. Mane, Cation distribution, magnetic properties and cubic perovskite phase transition in bismuth-doped nickel ferrite, Solid State Sci. 74 (2017) 88–94.
- [10] M. Menzel, V. Sepalak, K.D. Becker, Mechanochemical reduction of nickel ferrite, Solid State Ionics 141-142 (2001) 663–669.
- [11] M. Sorescu, L. Diamandescu, P.D. Ramesh, R. Roy, A. Daly, Z. Bruno, Evidence for microwave-induced recrystallization in NiZn ferrites, Mater. Chem. Phys. 101 (2007) 410–414.
- [12] M.A. Gabal, Y.M. Al Angari, Effect of diamagnetic substitution on the structural, magneticand electrical properties of NiFe₂O₄, Mater. Chem. Phys. 115 (2009) 578–584.
- [13] N.A.S. Nogueira, V.H.S. Utuni, Y.C. Silva, P.K. Kiyohara, I.F. Vasconcelos, M.A.R. Miranda, J.M. Sasaki, X-ray diffraction and Mössbauer studies on superparamagnetic nickel ferrite obtained by proteic sol-gel method, Mater. Chem. Phys. 163 (2015) 402–406.
- [14] M.V. Ushakov, B. Senthikumar, R.K. Selvan, I. Felner, M.I. Oshtrakh, Mössbauer spectroscopy of NiFe₂O₄ nanoparticles: the effect of Ni²⁺ in the Fe³⁺ microenvironment in both tetrahedral and octahedral sites, Mater. Chem. Phys. 202 (2017) 159–168.
- [15] Aakash, A. Roychowdhury, D. Das, S. Mukerjee, Effect of doping of chromium ions on the structural and magnetic properties of nickel ferrite, Ceram. Int. 42 (2016) 7742, 7747.
- [16] M.K. Anupama, N. Srinatha, S. Matteppanavar, B. Angadi, B. Sahoo, B. Rudraswamy, Effect of zinc substitution on the structural and magnetic properties of nanocrystalline NiFe₂O₄ ferrites, Ceram. Int. 44 (2018) 4946-4054.
- [17] M.H. Mahmoud, H.H. Hamdeh, J.C. Ho, M.J. O'Shea, J.C. Walker, Mössbauer studies of manganese ferrite fine particles processed by ball milling, J. Magn. Magn. Mater. 220 (2000) 139–146.
- [18] E.C. Sousa, M.H. Sousa, G.F. Goya, H.R. Rechenberg, M.C.F.L. Lara, F.A. Tourinho, J. Depeyrot, Enhanced surface anisotropy evidence by Mössbauer spectroscopy in nickel ferrite nanoparticles, J. Magn. Magn. Mater. 272-276 (2004) e1215–e1217.

- [19] V. Sepelak, M. Manzel, I. Bergmann, M. Wiebcke, F. Krumeich, K.D. Becker, Structural and magnetic properties of nanosize mechanosythesized nickel ferrite, J. Magn. Magn. Mater. 272-276 (2004) 1616–1618.
- [20] A. Alawat, V.G. Sathe, V.R. Reddy, A. Gupta, Mössbauer, Raman and X-ray diffraction studies of superparamagnetic NiFe₂O₄ nanoparticles prepared by sol-gel auto-combustion method, J. Magn. Magn. Mater. 323 (2011) 2049–2054.
- [21] M.H. Mahmoud, A.M. Elshahawy, S.A. Maklouf, H.H. Hamdeh, Mössbauer and magnetization studies of nickel ferrite nanoparticles synthesized by the microwave combustion method, J. Magn. Magn. Mater. 343 (2013) 21–26.
- [22] R. Galindo, N. Menendez, P. Crespo, V. Velasco, O. Bomati-Miguel, D. Diaz-Fernandez, P. Herrasti, Comparison of different methodologies for obtaining nickel nanoferrites, J. Magn. Magn. Mater. 361 (2014) 118–125.
- [23] V.K. Chakradhary, A. Ansari, M.J. Akhtar, Design, synthesis and testing of high coercivity cobalt doped nickel ferrite nanoparticles for magnetic applications, J. Magn. Magn. Mater. 469 (2019) 674–680.
- [24] H. Salazaar-Tamayo, K.E. Garcia, C.A. Barrero, New method to calculate Mössbauer recoilless f-factors in NiFe₂O₄. Magnetic, morphological and structural properties, J. Magn. Magn. Mater. 471 (2019) 242–249.
- [25] C.A.P. Gomez, C.A. Barrero Meneses, J.A. Jaen, Raman, infrared and Mössbauer spectroscopic studies of solid state synthesized Ni-Zn ferrites, J. Magn. Magn. Mater. 505 (2020) 166710.
- [26] M. Siddique, N.M. Butt, Effect of particle size on degree of inversion in ferrites investigated by Mössbauer spectroscopy, Physica B 405 (2010) 4211–4215.
- [27] Aakash, R. Choubey, D. Das, S. Mukherjee, Effect of doping of manganese ions on the structural and magnetic properties of nickel ferrite, J. Alloys Compd. 668 (2016) 33–39.
- [28] T.P. Poudel, B.K. Rai, S. Yoon, D. Guragain, D. Neupane, S.R. Mishra, The effect of gadolinium substitution in inverse spinel ferrite: structural, magnetic and Mössbauer study, J. Alloys Compd. 802 (2019) 609–619.
- [29] J.A.C. Arango, A.A. Cristobal, C.P. Ramos, P.G. Bercoff, P.M. Botta, Mechanochemical synthesis and characterization of nanocrystalline Ni-Co ferrites, J. Alloys Compd. 811 (2019) 152044.
- [30] V.A. Bharati, S.B. Somvanshi, A.V. Humbe, V.D. Murumkar, V.V. Sondur, K.M. Jadhav, Influence of trivalent Al-Cr co-substitution on the structural, morphological and Mössbauer properties of nickel ferrite nanoparticles, J. Alloys Compd. 821 (2020) 153501.
- [31] I. Sabikoglu, L. Parali, O. Malina, P. Novak, J. Kaslik, J. Tucek, J. Pechousek, J. Navarik, O. Schneeweiss, The effect of neodymium substitution on the structural and magnetic properties of nickel ferrite, Prog. Nat. Sci. Mater. Int. 25 (2015) 215–221
- [32] R. Swaminathan, S. Calvin, M. Sorescu, L. Diamandescu, M.E. McHenry, Surface structure model of cuboctahedrally truncated ferrite nanoparticles, Int. Conf. Ferrites Am. Ceram. Soc. 9 (2005) 847–852 (ISBN 9781574982183).
- [33] R. Swaminathan, M.E. McHenry, P. Poddar, H. Srikant, Magnetic properties of polydisperse and monodisperse NiZn ferrite nanoparticles interpreted in a surface structure model, J. Appl. Phys. 97 (2005) 10G104–10G104-3.
- [34] S.-J. Son, M. Taheri, E.E. Carpenter, V.G. Harris, M.E. McHenry, Synthesis of ferrite and nickel ferrite nanoparticles using radio-frequency thermal plasma torch, J. Appl. Phys. 91 (2002) 7589–7591.
- [35] Monica Sorescu, Recent Applications of the Mössbauer Effect, Dorrance Publishing Company, Pittsburgh, 2020 (ISBN 9781646104970).
- [36] M. Sorescu, A new method for direct determination of the recoilless fraction using a single room-temperature Mössbauer measurement of a two-foil absorber, Mater. Lett. 54 (2002) 256–259.
- [37] M. Sorescu, M. Knauss, A. Perrin, M. McHenry, Zero-dimensional graphene and its behavior under mechanochemical activation with zinc ferrite nanoparticles, MRS Adv., (in press).
- [38] G.A. Sawatzky, F. van der Woude, A.H. Morrish, Recoilless ratios for ⁵⁷Fe in octahedral and tetrahedral sites of a spinel and a garnet, Phys. Rev. 183 (1969) 383–386
- [39] M. Sorescu, Introducing Mossbauer spectroscopy to undergraduate students, J. Mater. Educ. 25 (2003) 143–150.